Protonation of *trans*-[Mo(η^2-MeCCH)$_2$($Ph_2PCH_2CH_2PPh_2$)$_2$]: Mechanism of Formation of *trans*-[MoX(CHCHMe)($Ph_2PCH_2CH_2PPh_2$)$_2$] (X = Cl or Br) or *trans*-[MoF(CCH_2Me)($Ph_2PCH_2CH_2PPh_2$)$_2$]

Richard A. Henderson,* Kay E. Oglieve and Philip Salisbury
John Innes Centre, Nitrogen Fixation Laboratory, University of Sussex, Brighton BN1 9RQ, UK

The reaction between *trans*-[Mo(η^2-MeCCH)$_2$($Ph_2PCH_2CH_2PPh_2$)$_2$] and an excess of anhydrous HX (X = Cl or Br) in tetrahydrofuran gives *trans*-[MoX(CHCHMe)($Ph_2PCH_2CH_2PPh_2$)$_2$] and the evolution of 1 mol equivalent of MeCCH. Mechanistic studies indicated that initial protonation of *trans*-[Mo(η^2-MeCCH)$_2$($Ph_2PCH_2CH_2PPh_2$)$_2$] occurs at a propyne ligand to form the vinyl species, *trans*-[Mo(CHCHMe)(η^2-MeCCH)($Ph_2PCH_2CH_2PPh_2$)$_2$]$^+$, and at low concentrations of acid rate-limiting dissociation of the other *trans*-propyne, followed by attack of halide ion at the molybdenum, produces *trans*-[MoX(CHCHMe)($Ph_2PCH_2CH_2PPh_2$)$_2$]. At high concentrations of acid further rapid protonation of the vinyl ligand occurs to give *trans*-[Mo($CHCH_2Me$)(η^2-MeCCH)($Ph_2PCH_2CH_2PPh_2$)$_2$]$^{2+}$. This second protonation further labilises the *trans*-propyne which is lost in the rate-limiting step and subsequent attack of halide gives *trans*-[MoX($CHCH_2Me$)($Ph_2PCH_2CH_2PPh_2$)$_2$]$^+$. Dissociation of a proton gives the product, *trans*-[MoX(CHCHMe)($Ph_2PCH_2CH_2PPh_2$)$_2$]. The reaction between *trans*-[Mo(η^2-MeCCH)$_2$($Ph_2PCH_2CH_2PPh_2$)$_2$] and HBF_4·OEt_2 gives a mixture of *trans*-[MoF(CHCHMe)($Ph_2PCH_2CH_2PPh_2$)$_2$] and the alkylidyne complex. *trans*-[MoF(CCH_2Me)($Ph_2PCH_2CH_2PPh_2$)$_2$]. The alkylidyne complex has been isolated pure by fractional crystallisation. The factors which discriminate between the formation of the vinyl and alkylidyne species are discussed.

Recently we have been interested in the protonation of unsaturated hydrocarbon residues co-ordinated to electron-rich metal sites,[1-6] not only to understand the rates and sites of the protonation in these systems,[7] but also to define the manner in which these protonations can control which hydrocarbons (alkanes, alkenes or alkynes) are subsequently released from the site.

Co-ordinated alkynes are of particular interest with respect to the manner in which protonation can produce stereospecific *cis* or *trans* alkenes: a reaction which is of fundamental importance both in synthetic chemistry and in understanding the non-physiological reactions of the metalloenzymes nitrogenases.[8,9] In this paper we report studies on the protonation of *trans*-[Mo(η^2-MeCCH)$_2$(dppe)$_2$] (dppe = $Ph_2PCH_2CH_2PPh_2$) with anhydrous HX (X = Cl, Br or BF_4) in tetrahydrofuran (thf) to give the corresponding vinyl and alkylidyne complexes as shown in Fig. 1.

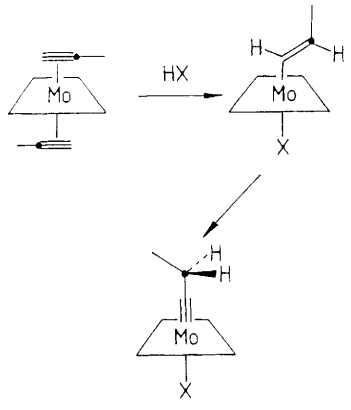

Fig. 1 Transformation of co-ordinated alkyne to a vinyl and alkylidyne species

Experimental

All manipulations in both the preparative and mechanistic aspects of this work were routinely performed under an atmosphere of dinitrogen or argon using standard Schlenk or syringe techniques as appropriate. Solvents were dried over the appropriate drying agent and distilled from that drying agent immediately prior to use: thf (Na–benzophenone), MeOH [$Mg(OMe)_2$], CH_2Cl_2 (K_2CO_3), Et_2O (Na). The reagents $SiClMe_3$ (Aldrich), MeOD (Aldrich), $MoCl_5$ (Aldrich) and propyne (BDH) were used as received; $Ph_2PCH_2CH_2PPh_2$ (Aldrich) was recrystallised from hot acetone prior to use.

trans-[Mo(N_2)$_2$(dppe)$_2$] was prepared by the literature method.[10]

Preparations.—*trans*-[Mo(η^2-MeCCH)$_2$(dppe)$_2$]. This complex was prepared by a method analogous to that described for *trans*-[Mo(η^2-PhCCH)$_2$(dppe)$_2$].[11]

Propyne was passed through a stirred suspension of *trans*-[Mo(N_2)$_2$(dppe)$_2$] (2.0 g, 2.1 mmol) in thf (*ca.* 100 cm^3) in a 500 cm^3 Schlenk flask for about 5 min, and the solution then stirred under an atmosphere of propyne for 24 h. During the first two or three hours of this period (when the colour of the solution was changing rapidly from orange to yellow-green) the atmosphere of propyne was replenished 2 or 3 times. After 24 h the solution was filtered through Celite to remove a small amount of insoluble material. The filtrate was concentrated *in vacuo* to *ca.* 30 cm^3, and addition of diethyl ether (*ca.* 100 cm^3) precipitated the product as a yellow solid, which was removed by filtration, washed with diethyl ether then dried *in vacuo*. The crude product is analytically clean but can be recrystallised at room temperature by rapid dissolution in propyne-saturated thf, followed by addition of propyne-saturated diethyl ether. Yield = 1.2 g, 58%.

trans-[MoX(CHCHMe)(dppe)$_2$] (X = Cl *or* Br). To a suspension of *trans*-[Mo(η^2-MeCCH)$_2$(dppe)$_2$] (0.3 g, 0.31 mmol) in thf (*ca.* 50 cm^3) was added MeOH (1.0 cm^3, 30 mmol), then $SiXMe_3$ (3.2 cm^3, 30 mmol, X = Cl or Br). The solution rapidly turned orange-red and became homogeneous whilst evolving a gas (propyne). After stirring for 30 min the solution was concentrated *in vacuo* to *ca.* 20 cm^3, then filtered through Celite to remove a small amount of insoluble material. Addition of diethyl ether (*ca.* 50 cm^3) to the filtrate precipitated the product as an orange (X = Cl) or orange-red (X = Br) solid which was removed by filtration, washed with diethyl ether then dried *in vacuo*. Recrystallisation can be accomplished by dissolving the complex in the minimum of dichloromethane followed by the addition of diethyl ether to precipitate the product. Yield = 0.2 g, 67%.

trans-[MoF(CCH_2Me)(dppe)$_2$]. To a suspension of *trans*-[Mo(η^2-MeCCH)$_2$(dppe)$_2$] (0.3 g, 0.31 mmol) in thf (*ca.* 50 cm^3) was added HBF_4·OEt_2 (1.0 cm^3, mmol). The mixture rapidly became red and homogeneous whilst evolving propyne. After stirring for 30 min all volatiles were removed *in vacuo*. The oily residue was extracted into dichloromethane (*ca.* 20 cm^3), then diethyl ether was layered carefully on top of the solution. Overnight red microcrystals of the product were deposited. The ^{1}H NMR spectrum of the crude product indicated that a mixture of alkylidyne and vinyl complexes (broad peaks δ 9.6 and 11.2 presumably due to *trans*-[MoF(CHCHMe)(dppe)$_2$]) were present. One or, occasionally, two recrystallisations from dichloromethane–diethyl ether gave a pure sample of the alkylidyne. Yield = 0.12 g, 42%.

Elemental analyses and spectroscopic characterisation of all these complexes are shown in Table 1.

Kinetic Studies.—The kinetics of all the reactions of *trans*-[Mo(η^2-MeCCH)$_2$(dppe)$_2$] with acids were studied under pseudo-first order conditions {[HX]:[Mo(η^2-MeCCH)$_2$(dppe)$_2$] ≥ 10:1} on a Hi-Tech SF-51 stopped-flow spectrophotometer modified to handle air-sensitive solutions.[12] The temperature was maintained at 25.0 °C using a Grant LE8 thermostat tank. The data were collected, analysed and stored on a Viglen 486 computer interfaced to the stopped-flow apparatus *via* an analogue-to-digital converter.

Stock 0.1 mol dm^{-3} solutions of anhydrous HCl or HBr for the kinetic studies were prepared by mixing equimolar amounts of MeOH and $SiXMe_3$ in thf. Dilute solutions of acid were prepared from this stock. All acid solutions were used within 1 h of preparation to minimise any acid-catalysed decomposition of thf.

Solutions of the complex were prepared under an atmosphere of argon, and used within 30 min to minimise dissociation of the propyne ligands (see below).

The ionic strength of the solutions was maintained at 0.1 mol dm^{-3} using [NBu^n_4]BF_4. Independent studies on these systems showed that the reaction rate and absorbance changes were identical in the presence and absence of [NBu^n_4]BF_4.

The stopped-flow traces were analysed on the computer by a program which fitted the curves to a defined, minimum number of exponentials. The dependence on the concentration of acid was established graphically in the usual manner.[13]

GLC Experiments.—In a typical experiment, *trans*-[Mo(η^2-MeCCH)$_2$(dppe)$_2$] (10.0 mmol dm^{-3}) was prepared in thf (10 cm^3) in a flask and sealed with a rubber septum. A known concentration of HX was introduced through the septum using a syringe. After stirring for *ca.* 5 min a sample of the gas (0.05 cm^3) within the flask was taken, using a syringe. The gas was analysed using a Philips PU4400 Gas Liquid Chromatograph, equipped with a Poropak Q column operating at 130 °C, and connected to a Philips computing integrator PU4815. Under all conditions propyne was the only gaseous product and was identified by comparison with the retention time of an authentic sample of propyne (retention time = 1.91 ± 0.01 min).

Spectroscopic Studies.—IR spectra were recorded on a Perkin-Elmer 883 spectrometer as KBr discs and UV/VIS spectra were recorded on a Shimadzu UV-2101PC spectrophotometer; ^{1}H, ^{31}P-{^{1}H} and ^{13}C-{^{1}H} NMR spectra together with the distortionless enhancement by polarisation transfer (DEPT) spectra were recorded on a JEOL GSX270 spectrometer.

Monitoring the Reaction by NMR Spectroscopy at Low Temperature.—The reactions between *trans*-[Mo(η^2-MeCCH)$_2$(dppe)$_2$] and anhydrous HX (X = Cl or Br) were monitored at −80 °C using ^{31}P-{^{1}H} NMR spectroscopy analogous to the method described earlier for studying ^{1}H NMR spectra.[14] A frozen sample containing a known concentration of complex dissolved in thf (typically 10.0 mmol dm^{-3}) was prepared at −170 °C in a 10 mm NMR tube, then a known volume of a standard acid solution was frozen on top of this material. After transferring this sample into the probe of the NMR spectrometer at −170 °C the solution was warmed to −80 °C, and the spectrum recorded at regular intervals. Examples of the spectra recorded are shown in Fig. 4.

Results and Discussion

Characterisation of the Complexes.—It has been shown previously[11] that the reaction of *trans*-[M(N_2)$_2$(dppe)$_2$] (M = Mo or W) with a range of alkynes (RCCH) gives the species *trans*-[M(η^2-PhCCH)$_2$(dppe)$_2$], *trans*-[MH_2(CCR)$_2$(dppe)$_2$] or *trans*-[M(CCR)$_2$(dppe)$_2$] (R = Ph, CO_2Me or CO_2Et). Protonation of these complexes with HBF_4 gives alkylidene or alkylidyne complexes which have been isolated and characterised for *trans*-[WF($CHCH_2Ph$)(dppe)$_2$]BF_4 and *trans*-[WF(CCH_2CO_2Me)(dppe)$_2$], respectively. However, the mechanisms by which these transformations of the co-ordinated alkyne are accomplished have not been established. In this paper we report the study of the protonation reactions of *trans*-[Mo(η^2-MeCCH)$_2$(dppe)$_2$] and define some of the factors which discriminate between the formation of vinyl and alkylidyne species shown in Fig. 1. The choice of the propyne complex was made deliberately since any hydrocarbon liberated in the reaction (whether it be propyne, propene or propane) is easily, quantitatively detectable using GLC.

trans-[Mo(η^2-MeCCH)$_2$(dppe)$_2$] was prepared by displacement of dinitrogen in *trans*-[M(N_2)$_2$(dppe)$_2$], and characterised by elemental analysis together with ^{1}H and ^{31}P-{^{1}H} NMR spectroscopies. IR spectroscopy was not particularly diagnostic for this material, but the absence of a strong band *ca.* 2000 cm^{-1} associated with ν(C≡C) demonstrates that the material is not an alkynyl complex.

In dinitrogen-saturated thf solutions *trans*-[Mo(η^2-MeCCH)$_2$(dppe)$_2$] loses propyne over the course of 2–3 h and forms *trans*-[M(N_2)$_2$(dppe)$_2$]. This observation, together with the relatively poor solubility of *trans*-[Mo(η^2-MeCCH)$_2$(dppe)$_2$] in solvents with which it does not react, meant we were unable to record the ^{13}C-{^{1}H} NMR spectrum of this complex. Even under an atmosphere of propyne significant decomposition occurred over the protracted times necessary to record the ^{13}C-{^{1}H} NMR spectrum.

The reaction of *trans*-[Mo(η^2-MeCCH)$_2$(dppe)$_2$] with an excess of anhydrous HX (X = Cl or Br) in thf gives the vinyl complexes, *trans*-[MoX(CHCHMe)(dppe)$_2$] as described by equation (1). The 1 mol equivalent of propyne that is liberated

trans-[Mo(η^2-MeCCH)$_2$(dppe)$_2$] + HX ⟶
trans-[MoX(CHCHMe)(dppe)$_2$] + MeCCH (1)

was identifed by GLC.

Table 1 Physical properties of the complexes

Complex	Elemental analysis[a] (%) C	H	UV/VIS[b]	Spectroscopic data ^{1}H[c]	^{31}P-{^{1}H}[d]	^{13}C-{^{1}H}[c]	Other
[Mo(η^2-MeCCH)$_2$(dppe)$_2$]	72.3 (71.6)	5.8 (5.8)	330 (7.2) 380 (5.2)	1.73 (s, *Me*CCH) 2.50 (s, MeCC*H*)	−81.6 (s)		
[MoCl(CHCHMe)(dppe)$_2$]·thf	68.2 (68.0)	5.5 (5.9)	358 (2.9) 410 (1.5)	11.2 (br, C*H*CHMe) 9.5 (br, CHC*H*Me) 3.7 (s, thf) 1.8 (s, thf) 1.7 (s, CHCH*Me*)	−92.1 (s)	163.2 (*C*HCHMe) 135–125 (m, *Ph*) 112.3 (CH*C*HMe) 65.8 (thf) 29.7 (P*C*H$_2$*C*H$_2$P) 25.7 (thf) 12.1 (CHCH*Me*)	+[e] + + − − − +
[MoBr(CHCHMe)(dppe)$_2$]·thf	65.1 (65.2)	5.5 (5.6)	380 (3.2) 430 (3.3)	10.9 (d, C*H*CHMe, J_{HH} = 8.8 Hz) 9.5 (m, CHC*H*Me) 3.7 (s, thf) 1.8 (s, thf) 1.15 (d, CHCH*Me*, J_{HH} = 5 Hz)	−103 (s)	163.0 (*C*HCHMe) 135–125 (m, *Ph*) 119 (CH*C*HMe) 65.8 (thf) 28.0 (P*C*H$_2$*C*H$_2$P) 25.7 (thf) 15.0 (CHCH*Me*)	
[MoF(CCH$_2$Me)(dppe)$_2$][f]	68.5 (69.3)	5.6 (5.6)		3.43 (q, CC*H*$_2$Me, J_{HH} = 6.7 Hz) 1.15 (t, CCH$_2$*Me*, J_{HH} = 6.7 Hz)	−100.7 (d, J_{PF} = 40.1 Hz)	250 (br, *C*CH$_2$Me) 135–125 (m, *Ph*) 29.7 (P*C*H$_2$*C*H$_2$P) 28.8 (*C*CH$_2$Me) 11.7 (CCH$_2$*Me*)	

[a] Calculated values shown in parentheses. [b] Values of λ_{max}/nm; molar absorption coefficients ($10^{-3}\varepsilon$/dm^3 mol^{-1} cm^{-1}) are given in parentheses. [c] Measured in CD_2Cl_2, chemical shifts in ppm relative to $SiMe_4$, all spectra show peaks attributable to Ph (6.5–7.4) and PCH_2CH_2P (2.2–2.8). s = Singlet, d = doublet, t = triplet, q = quartet, qnt = quintet, m = multiplet, br = broad. [d] Measured in thf, chemical shifts in ppm relative to $P(OMe)_3$. [e] Orientation of resonance in DEPT spectrum. [f] Fluorine-19 NMR spectrum, measured in thf, chemical shift in ppm relative to $CFCl_3$. δ −121 (qnt, J_{FP} = 40.3 Hz).

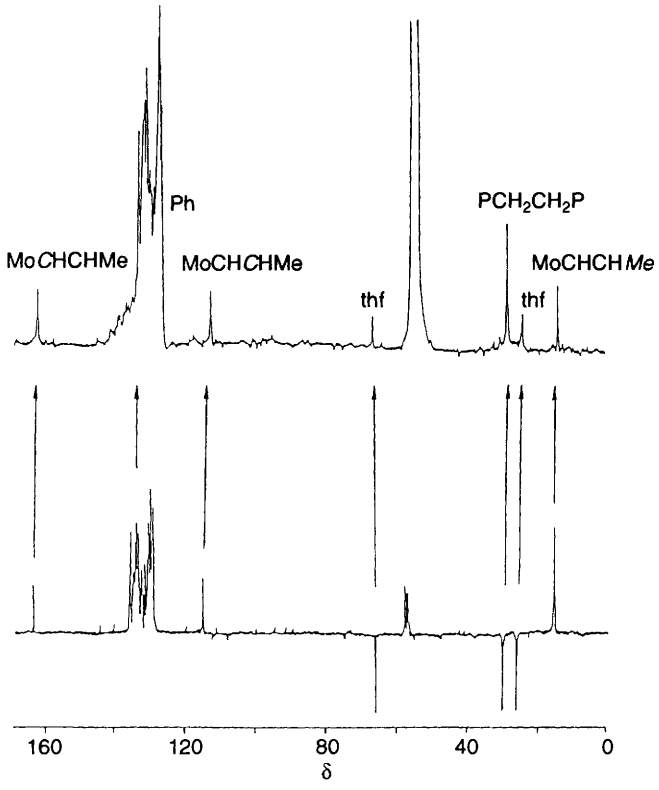

Fig. 2 Correlation of the ^{13}C-$\{^1H\}$ and DEPT NMR spectra of *trans*-[MoCl(CHCHMe)(dppe)$_2$] recorded at 25.0 °C in CD_2Cl_2

Fig. 3 Proton NMR spectrum of *trans*-[MoBr(CHCHMe)(dppe)$_2$] showing the partially resolved vinyl resonances, recorded at 25.0 °C in CD_2Cl_2

The vinyl complexes were isolated and characterised by elemental analysis, together with ^1H, ^{31}P-$\{^1H\}$ and ^{13}C-$\{^1H\}$ NMR spectroscopies. DEPT NMR spectroscopy was used to confirm the assignments of the ^{13}C-$\{^1H\}$ NMR spectrum (Fig. 2). Again IR spectroscopy is not diagnostic for this class of compound.

In the ^1H NMR spectrum the resonances attributable to the vinyl ligand in *trans*-[MoCl(CHCHMe)(dppe)$_2$] (δ 9.5 and 11.2) are broad and contain no structure. However, for the bromo-analogue these signals are at least partially resolved, as shown in Fig. 3, with the resonance at δ 10.9 appearing as a doublet, J_{HH} = 8.8 Hz, and the resonance at δ 9.5 being a multiplet. In addition the methyl signal at δ 1.15 is a doublet, J_{HH} = 5 Hz. The spectrum does not change appreciably in the temperature range −40 to +40 °C.

These coupling constants are consistent with a *cis* geometry for the vinyl ligand, since in organic molecules the proton spin–spin coupling constants[15] for *cis*-vinyl residues are J_{HH} = 6–14 Hz and for *trans*-vinyl residues J_{HH} = 11–20 Hz. In addition the coupling constant for the methyl group to the hydrogen on the adjacent carbon atom falls in the expected range, J_{HH} = 4–10 Hz. We will return to the origins of this stereochemistry after we have discussed the mechanism by which these vinyl species are formed.

Although the complexes, *trans*-[MoX(CHCHR)(dppe)$_2$] have not been reported before the similar species, [MoH$_2$(CHCHR)(dppe)$_2$]$^+$ and [MoH$_2$Br(CHCHR)(dppe)$_2$] (R = Me or Et) have been prepared[16] by the reaction of HCCCO$_2$R with [MoH$_4$(dppe)$_2$] in the presence of HBr, and the spectroscopic characteristics of these complexes are very similar to those of the compounds reported herein. Dihydrogen does not react at room temperature with [MoBr(CHCHMe)(dppe)$_2$] to produce [MoH$_2$Br(CHCHMe)(dppe)$_2$].

The crude product from the reaction of *trans*-[Mo(η^2-MeCCH)$_2$(dppe)$_2$] with HBF$_4$·OEt$_2$ is a mixture of a vinyl species {presumably *trans*-[MoF(CHCHMe)(dppe)$_2$]} and the alkylidyne complex, *trans*-[MoF(CCH$_2$Me)(dppe)$_2$] (see Experimental section). We have been able to isolate and fully characterise only the pure alkylidyne from this mixture by repeated fractional recrystallisation.

The alkylidyne is readily distinguished from the isomeric vinyl species by the characteristic resonances in the ^1H NMR spectrum attributable to the ethyl ligand (see Table 1), and the low-field resonance in the ^{13}C-$\{^1H\}$ NMR spectrum at δ 250.0 in the region characteristic of alkylidyne complexes (δ 230–320).[11]

Mechanism of Protonation of trans-[Mo(η^2-MeCCH)$_2$(dppe)$_2$].—The mechanism of the rapid reactions between *trans*-[Mo(η^2-MeCCH)$_2$(dppe)$_2$] and anhydrous HX (X = Cl, Br or BF$_4$) have been studied using stopped-flow spectrophotometry. In addition, low-temperature ^{31}P-$\{^1H\}$ NMR spectroscopy has been used to obtain structural information about a common intermediate detected in the reactions with HCl and HBr. Since this structural information is crucial in establishing the initial sites of protonation of the propyne complex the NMR spectroscopic experiments will be described before the kinetic analyses.

Detection of an Intermediate in the Protonation of trans-[Mo(η^2-MeCCH)$_2$(dppe)$_2$].—Shown in Fig. 4 is a series of ^{31}P-$\{^1H\}$ NMR spectra recorded at low temperatures during the reaction between the propyne complex and 2 mol equivalents of anhydrous HCl in thf.

Even in the first spectrum (recorded after *ca.* 10 min) the peak attributable to *trans*-[Mo(η^2-MeCCH)$_2$(dppe)$_2$] (δ −81.6, s) is much diminished, and a new singlet resonance has appeared at δ −62.2. This new peak grows in intensity progressively as the resonance due to the propyne complex decreases. At −80 °C the resonance at δ −62.2 only slowly decreases in intensity (over several hours). However, if the solution is warmed to −20 °C then this peak decreases in intensity as a resonance attributable to *trans*-[MoCl(CHCHMe)(dppe)$_2$] (δ −92.1, s)

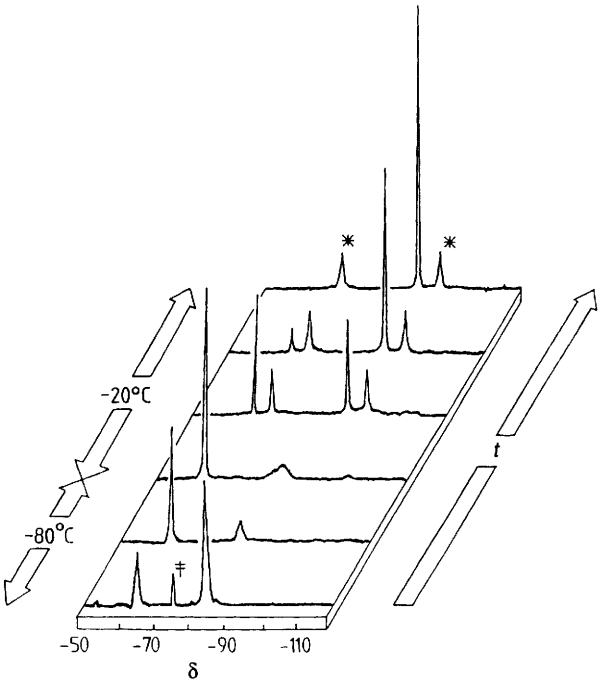

Fig. 4 $^{31}P-\{^{1}H\}$ NMR spectra of the reaction between *trans*-[Mo(η^2-MeCCH)$_2$(dppe)$_2$] (10.0 mmol dm^{-3}) and HCl (20.0 mmol dm^{-3}) recorded in thf. The resonance at δ −75.1 (‡) is due to traces of *trans*-[Mo(N$_2$)$_2$(dppe)$_2$], formed by substitution of the propyne complex prior to acidification. The resonances at δ −70.4 (*) and −97.2 (*) are attributable[2] to [MoH$_2$Cl$_2$(dppe)$_2$] formed by protonation of the dinitrogen complex[12]

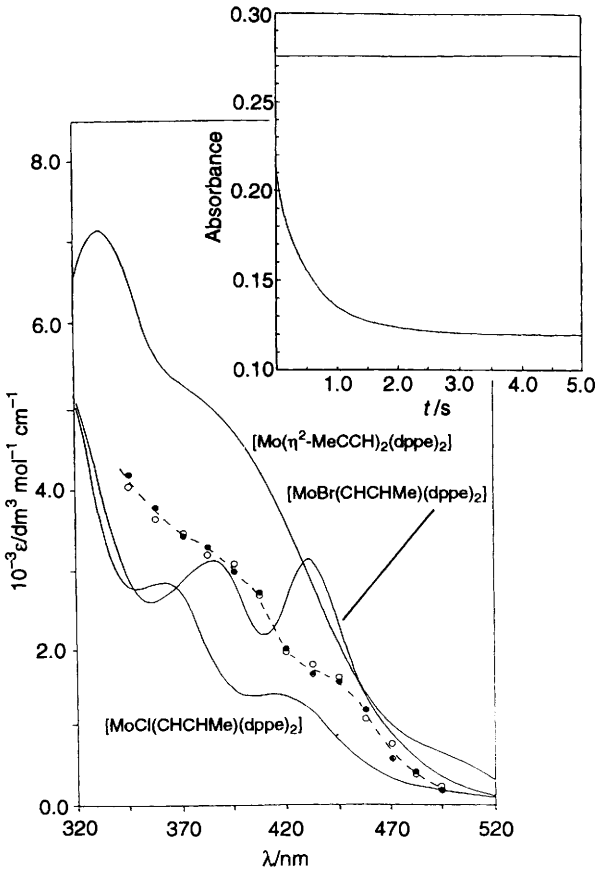

Fig. 5 UV/VIS absorption spectra of *trans*-[Mo(η^2-MeCCH)$_2$(dppe)$_2$], *trans*-[MoBr(CHCHMe)(dppe)$_2$] and *trans*-[MoCl(CHCHMe)(dppe)$_2$]. Also shown is the spectrum of the intermediate, *trans*-[Mo(CHCHMe)(η^2-MeCCH)(dppe)$_2$]$^+$, measured on the stopped-flow apparatus in the reactions with HCl (●) and HBr (○). All spectra were recorded in thf at 25.0 °C. (Insert) Stopped-flow absorbance–time trace for the reaction between *trans*-[Mo(η^2-MeCCH)$_2$(dppe)$_2$] (0.05 mmol dm^{-3}) and HBr (5.0 mmol dm^{-3}), measured in thf at 25.0 °C {ionic strength = 0.1 mol dm^{-3}, [NBu$^n_4$]BF$_4$}, λ = 360 nm. The curve is an excellent fit to a single exponential with k_{obs} = 1.8 s^{-1}, absorbance change = 0.08, and final absorbance = 0.120. Also shown is the absorbance of *trans*-[Mo(η^2-MeCCH)$_2$(dppe)$_2$] at 0.275

grows. In a similar experiment with 10 mol equivalents of HCl the position of the resonance attributable to this intermediate has shifted slightly to δ −64.4.

That the spectrum of the intermediate is a singlet demonstrates retention of the *trans*-Mo(dppe)$_2$ core for this species and, based on the results of the kinetics analysis (see below), we propose that at low concentrations of acid this intermediate (δ −62.2) is *trans*-[Mo(CHCHMe)(η^2-MeCCH)(dppe)$_2$]$^+$. At higher concentrations of acid, further protonation can occur and the resonance at δ −64.4 is an equilibrium mixture of *trans*-[Mo(CHCHMe)(η^2-MeCCH)(dppe)$_2$]$^+$ and *trans*-[Mo(CHCH$_2$Me)(η^2-MeCCH)(dppe)$_2$]$^{2+}$. These proposals are consistent with: (*i*) the spectrophotometric detection of this intermediate; (*ii*) that the same resonance is observed in analogous studies with HBr, at all acid concentrations (δ −65.0, s) and (*iii*) that the resonances shift slightly upon changing the acid concentration. It must be emphasised that these spectroscopic studies alone do not represent convincing evidence for the proposed equilibrium mixture of intermediates. However, the kinetic studies unambiguously demonstrate the formation of a mono- and diprotonated species (see below).

We have been unable to obtain a high quality ^{1}H NMR spectrum of this intermediate because: (*i*) signals from other protic species such as SiMe$_3$OCD$_3$, residual thf and CH$_n$D$_{3-n}$OD are present and (*ii*) the resolution of the spectrum is poor because we have to record the spectrum in a 10 mm NMR tube since 5 mm tubes break upon thawing the reaction solution in the probe of the NMR spectrometer. However, there is no obvious hydride signal at high field in the spectrum of the intermediate.

The kinetics of the reactions between *trans*-[Mo(η^2-MeCCH)$_2$(dppe)$_2$] and anhydrous HCl or HBr to form *trans*-[MoX(CHCHMe)(dppe)$_2$] have been studied, as have the kinetics of the reaction with HBF$_4$·OEt$_2$ to form a mixture of *trans*-[MoF(CHCHMe)(dppe)$_2$] and *trans*-[MoF(CCH$_2$Me)(dppe)$_2$]. In all cases the same fundamental mechanism operates but the observed rate laws are different because of various limiting forms of the generalised rate law with the different acids. Consequently the reaction with HBr will be discussed first, then the reaction with HCl and finally the reaction with HBF$_4$·OEt$_2$. In this way it will be seen, in a logical manner, how the values of the elementary rate constants derived in the studies with HBr can be used to assist the more complex analysis of the kinetics with HCl.

Formation of trans-[MoBr(CHCHMe)(dppe)$_2$].—When studied on a stopped-flow spectrophotometer the reaction between *trans*-[Mo(η^2-MeCCH)$_2$(dppe)$_2$] and an excess of anhydrous HBr occurs in two distinct stages as shown by the stopped-flow absorbance–time trace in Fig. 5.

At λ ⩽ 420 nm the reaction is characterised by an initial absorbance decrease (which is complete within the dead time of the apparatus, 2 ms) to generate an intermediate, followed by an exponential absorbance decay to give *trans*-[MoBr(CHCHMe)(dppe)$_2$]. At λ > 420 nm the absorbance–time behaviour is slightly different and involves an initial absorbance decrease (complete within 2 ms) to generate the intermediate, followed by an absorbance increase. This difference in behaviour in the two wavelength ranges is merely a consequence of the relative absorbances of the intermediate and *trans*-[MoBr(CHCHMe)(dppe)$_2$] as shown in Fig. 5.

It seems likely that the intermediate detected on the stopped-flow apparatus at 25.0 °C has a single proton added to *trans*-[Mo(η^2-MeCCH)$_2$(dppe)$_2$]. This proposal has been confirmed in the studies with HCl (see below). In addition, it is this intermediate which is detected by low-temperature ^{31}P-{^{1}H} NMR spectroscopy and shown in Fig. 4. The visible absorption spectrum of the intermediate is shown in Fig. 5.

There are two sites on *trans*-[Mo(η^2-MeCCH)$_2$(dppe)$_2$] at which the protonation can occur: the metal to form [MoH(η^2-MeCCH)$_2$(dppe)$_2$]$^+$ or a propyne ligand to form [Mo(CHCHMe)(η^2-MeCCH)(dppe)$_2$]$^+$. The ^{31}P-{^{1}H} NMR spectrum of the intermediate demonstrates not only the *trans* geometry of the diphosphine chelates but also the singlet resonance indicates that protonation has not occurred at the metal, otherwise a more complicated AA'XX' pattern {as observed[1] in [WH(η^2-C$_2$H$_4$)$_2$(dppe)$_2$]$^+$}, or AA'BB' pattern {as observed[2] in [MoH(η^2-C$_2$H$_4$)$_2$(dppe)$_2$]$^+$} would result. That protonation of *trans*-[Mo(η^2-MeCCH)$_2$(dppe)$_2$] occurs most rapidly at the hydrocarbon ligand to form *trans*-[Mo(CHCHMe)(η^2-MeCCH)(dppe)$_2$]$^+$ is consistent with studies on the analogous *trans*-[M(η^2-C$_2$H$_4$)$_2$(dppe)$_2$] (M = Mo or W)[1,2] where the ethylene ligand is protonated at least 100 times faster than the metal.

The absorbance–time trace for the formation of *trans*-[MoBr(CHCHMe)(dppe)$_2$] from this intermediate can be satisfactorily fitted by a single exponential over the entire duration of the reaction. The exponential nature of this curve indicates that the reactions exhibit a first-order dependence on the concentration of the complex. This is confirmed by experiments performed at a constant concentration of [HBr] = 10 mmol dm^{-3}, whilst the concentration of *trans*-[Mo(η^2-MeCCH)$_2$(dppe)$_2$] is changed in the range 0.25–0.05 mmol dm^{-3}, under these conditions, k_{obs} = 2.1 ± 0.1 s^{-1}. Here and throughout this paper k_{obs} is the observed pseudo-first order rate constant measured under conditions where [HX] ≥ 10[Mo(η^2-MeCCH)$_2$(dppe)$_2$].

The dependence on the concentration of HBr is complicated as shown in Fig. 6.

At low concentrations of HBr the rate exhibits a first-order dependence on the concentration of acid, whereas at high concentrations of HBr the rate is independent of the concentration of acid. In addition, at low concentrations of HBr k_{obs} extrapolates, not to zero, but to a finite value. Analysis of these data by the usual graph[13] of $1/k_{obs}^{corr}$ against 1/[HBr] gives a straight line from which the rate law shown in equation (2) can be derived ($k_{obs}^{corr} = k_{obs} - 0.40$, *i.e.* correcting k_{obs} for the rate observed at low concentrations of HBr).

The rate of the reaction is unaffected by the use of DBr rather than HBr (see Fig. 6). These kinetics, together with the detection of the intermediate, *trans*-[Mo(CHCHMe)(η^2-MeCCH)(dppe)$_2$]$^+$ by both stopped-flow spectrophotometry and low-temperature ^{31}P-{^{1}H} NMR spectroscopy are consistent with the mechanism shown in Scheme 1.

Initial protonation of a propyne ligand in *trans*-[Mo(η^2-MeCCH)$_2$(dppe)$_2$] generates *trans*-[Mo(CHCHMe)(η^2-MeCCH)(dppe)$_2$]$^+$ in a reaction which is complete within the dead time of the stopped-flow apparatus even at the lowest concentration of HBr used, from which we can estimate the rate constant for protonation of the propyne as, $k_1^{Br} \geq 5 \times 10^5$ dm^3 mol^{-1} s^{-1}.

Protonation of a propyne ligand decreases the electron density at the metal and consequently labilises the *trans*-propyne ligand towards dissociation in the k_3 step. Subsequent rapid binding of Br$^-$ at the, thus generated, five-co-ordinate intermediate produces *trans*-[MoBr(CHCHMe)(dppe)$_2$]. At low concentration of HBr this is the exclusive product-forming pathway. However, at higher concentrations of HBr a further protonation of *trans*-[Mo(CHCHMe)(η^2-MeCCH)(dppe)$_2$]$^+$ occurs, and it seems most likely that this gives *trans*-[Mo(CHCH$_2$Me)(η^2-MeCCH)(dppe)$_2$]$^{2+}$. This second protonation of *trans*-[Mo(η^2-MeCCH)$_2$(dppe)$_2$] is reflected in the ^{31}P-{^{1}H} NMR spectrum of the intermediate by a slightly acid concentration dependent shift in the resonance position (see above). Formation of *trans*-[Mo(CHCH$_2$Me)(η^2-MeCCH)(dppe)$_2$]$^{2+}$ labilises the *trans*-propyne ligand which is lost in the rate-limiting k_4 step. Rapid attack by Br$^-$ at the five-co-ordinate intermediate gives *trans*-[MoBr(CHCH$_2$Me)(dppe)$_2$]$^+$. Subsequent dissociation of a proton from the carbon atom remote from the metal results in the product that is isolated, *trans*-[MoBr(CHCHMe)(dppe)$_2$]. This deprotonation need not be fast. Although the final absorbances measured in the stopped-flow experiments are those expected of *trans*-[MoBr(CHCHMe)(dppe)$_2$], it seems likely that in solution an equilibrium mixture of the four complexes shown on the right hand side of Scheme 1 is present. This aspect of the study will be discussed in more detail later.

The mechanism shown in Scheme 1 is consistent with the observed kinetics. A generalised rate law for the mechanism shown in Scheme 1 can be derived by assuming that K_1^X and K_2^X are both protonation equilibria, rapidly established prior to the rate-limiting dissociation of the propyne ligands in the k_3 and k_4 steps. The resulting rate law is shown in equation (3).

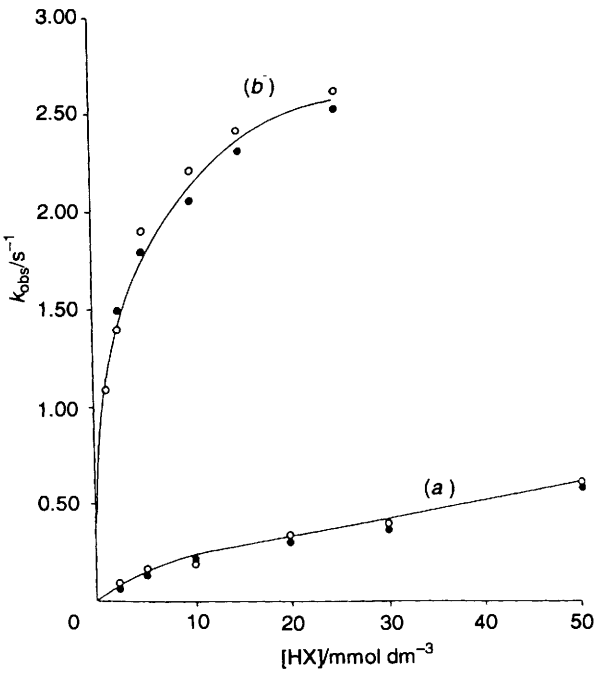

Fig. 6 Dependence of k_{obs} on the concentration of acid for the reaction between *trans*-[Mo(η^2-MeCCH)$_2$(dppe)$_2$] (0.05 mmol dm^{-3}) and anhydrous HCl (*a*) or HBr (*b*) in thf at 25.0 °C {ionic strength = 0.1 mol dm^{-3}, [NBu$^n_4$]BF$_4$}. Data points correspond to HX (●) and DX (○)

$$\frac{-d[Mo(\eta^2\text{-MeCCH})_2(dppe)_2]}{dt} = \frac{\{(0.40 \pm 0.05) + (1.26 \pm 0.1) \times 10^3[HBr]\}}{1 + (4.89 \pm 0.8) \times 10^2[HBr]} [Mo(\eta^2\text{-MeCCH})_2(dppe)_2] \quad (2)$$

$$\frac{-d[Mo(\eta^2\text{-MeCCH})_2(dppe)_2]}{dt} = \frac{K_1^X[HX]\{k_3 + K_2^X k_4[HX]\}}{1 + K_1^X[HX] + K_1^X K_2^X[HX]^2} [Mo(\eta^2\text{-MeCCH})_2(dppe)_2] \quad (3)$$

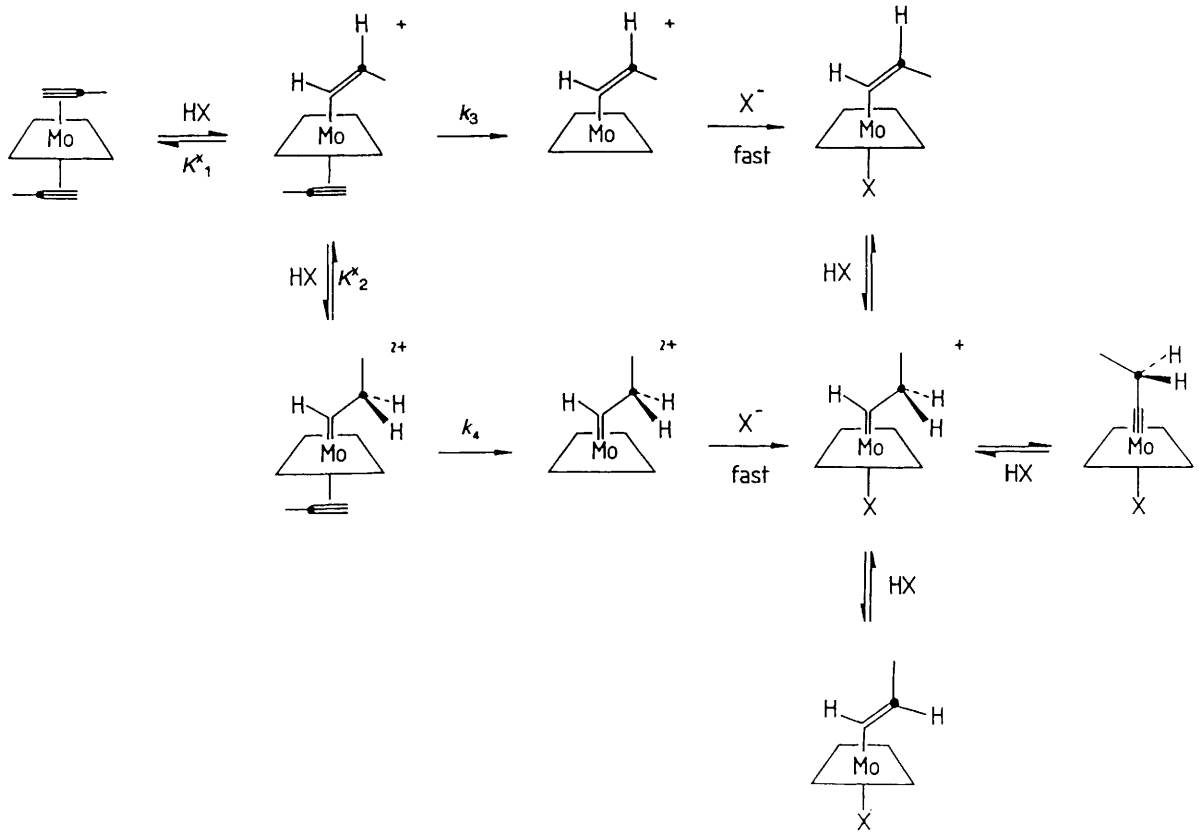

Scheme 1 Mechanism for the reactions of *trans*-[Mo(η^2-MeCCH)$_2$(dppe)$_2$] with anhydrous HX (X = Cl, Br or BF_4) in thf; diphosphine ligands omitted for clarity. The species, *trans*-[Mo(CHCHMe)(η^2-MeCCH)(dppe)$_2$]$^+$ and *trans*-[Mo(CHCH$_2$Me)(η^2-MeCCH)(dppe)$_2$]$^{2+}$ have been detected by both visible absorption spectroscopy (Fig. 5) and ^{31}P-{^{1}H} NMR spectroscopy (Fig. 4)

Table 2 Summary of elementary rate and equilibrium constants

Acid	K_1^X/dm^3 mol^{-1}	K_2^X/dm^3 mol^{-1}	k_3/s^{-1}	k_4/s^{-1}
HCl	1.3×10^2	3.0[a]	0.35	*a*
HBr	$\geqslant 1.9 \times 10^4$[b]	4.9×10^2	0.40	2.58
HBF_4				2.75

[a] This value is estimated since analysis of the data gives $K_2^{Cl}k_4 = 7.5$ dm^3 mol^{-1} s^{-1}, and $k_4 = 2.58$ s^{-1} (from analysis of the data with HBr), consequently we can calculate $K_2^{Cl} = 3.0$ dm^3 mol^{-1}. [b] This limit is established since even when [HBr] = 1.0 mmol dm^{-3} at least 95% of the *trans*-[Mo(η^2-MeCCH)$_2$(dppe)$_2$] is converted to *trans*-[Mo(CHCHMe)(η^2-MeCCH)(dppe)$_2$]$^+$ within the dead-time of the stopped-flow apparatus.

In the reaction with HBr a simplified expression is valid. Since *trans*-[Mo(CHCHMe)(η^2-MeCCH)(dppe)$_2$]$^+$ is formed within the dead-time of the stopped-flow apparatus the kinetics that are being monitored correspond to the decomposition of this species. Consequently $K_1^{Br}[HBr] \gg 1$, giving rise to equation (4).

$$\frac{-d[Mo(\eta^2\text{-MeCCH})_2(dppe)_2]}{dt} = \frac{\{k_3 + K_2^X k_4[HX]\}}{1 + K_2^X[HX]}[Mo(\eta^2\text{-MeCCH})_2(dppe)_2] \quad (4)$$

This expression is identical in form to that observed experimentally for the fast phase shown in equation (2), and comparison of equations (2) and (4) allows the determination of the elementary rate and equilibrium constants which are summarised in Table 2.

The reactivity of the protonated intermediates, *trans*-[Mo(CHCHMe)(η^2-MeCCH)(dppe)$_2$]$^+$ and *trans*-[Mo(CHCH$_2$Me)(η^2-MeCCH)(dppe)$_2$]$^{2+}$ deserves further comment. Both these species are co-ordinatively-unsaturated, formally sixteen-electron complexes, and consequently dissociation of the *trans*-propyne ligands would result in a five-co-ordinate, formally fourteen-electron species. It may be that, in order to avoid the relatively high-energy fourteen-electron species, halide ion may bind to the metal prior to, or synchronous with, propyne dissociation. The solvent thf has a low relative permittivity and this will favour tight ion-pairing between halide ion and the cationic complexes. Consequently, a halide ion may be in an advantageous position to attack the intermediates.

Formation of trans-[MoCl(CHCHMe)(dppe)$_2$].—When monitored on a stopped-flow apparatus the reaction between *trans*-[Mo(η^2-MeCCH)$_2$(dppe)$_2$] and anhydrous HCl shows marked differences in the absorbance–time behaviour to that observed for the reaction with HBr. In the wavelength range studied, λ = 350–480 nm, an absorbance decrease is observed, with the final absorbance corresponding to that of *trans*-[MoCl(CHCHMe)(dppe)$_2$]. However, the initial absorbance varies with the concentration of HCl. Thus at low concentrations of HCl the initial absorbance is that of *trans*-[Mo(η^2-MeCCH)$_2$(dppe)$_2$] but increasing the concentration of HCl results in progressively lower initial absorbances until, at [HCl] > 30 mmol dm^{-3}, further increase in the concentration of acid does not affect the initial absorbance. This behaviour is consistent with an equilibrium protonation of *trans*-[Mo(η^2-MeCCH)$_2$(dppe)$_2$] to form *trans*-[Mo(CHCHMe)(η^2-MeCCH)(dppe)$_2$]$^+$. Knowing the molar absorption coefficients for *trans*-[Mo(η^2-MeCCH)$_2$(dppe)$_2$] and *trans*-[Mo(CHCHMe)(η^2-MeCCH)(dppe)$_2$]$^+$ the value of $K_1^{Cl} = 1.3 \times 10^2$ dm^3 mol^{-1} can be determined graphically as shown in Fig. 7.

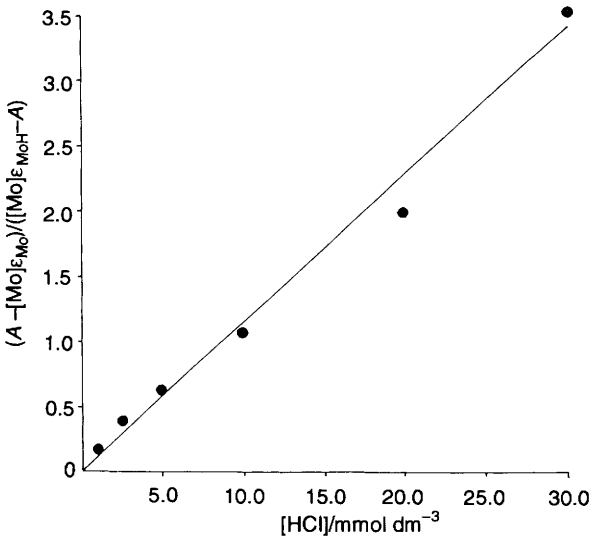

Fig. 7 Graphical determination of the equilibrium constant, K_1^{Cl}, for the reaction between *trans*-[Mo(η^2-MeCCH)$_2$(dppe)$_2$] and anhydrous HCl in thf at 25.0 °C {ionic strength = 0.1 mol dm^{-3}, [NBu$^n_4$]BF$_4$}, from analysis of the initial absorbance decrease measured on the stopped-flow apparatus at λ = 420 nm. The quotient, $(A - [Mo]\varepsilon_{Mo})/([Mo]\varepsilon_{MoH} - A)$ is the ratio of the equilibrium concentrations of *trans*-[Mo(CHCHMe)(η^2-MeCCH)(dppe)$_2$]$^+$Cl$^-$ to *trans*-[Mo(η^2-MeCCH)$_2$(dppe)$_2$] {A = initial absorbance of the stopped-flow trace, [Mo] = the initial concentration of *trans*-[Mo(η^2-MeCCH)$_2$(dppe)$_2$] (0.05 mmol dm^{-3}). ε_{Mo} = molar absorption coefficient of *trans*-[Mo(η^2-MeCCH$_2$)(dppe)$_2$] (3.68 × 10^3 dm^3 mol^{-1} cm^{-1}) and ε_{MoH} = molar absorption coefficient of *trans*-[Mo(CHCHMe)(η^2-MeCCH)(dppe)$_2$]$^+$ (1.70 × 10^3 dm^3 mol^{-1} cm^{-1}); ε_{Mo} and ε_{MoH} were determined from the initial absorbances of the stopped-flow traces at [HCl] = 0.0 mmol dm^{-3} and [HCl] = 50.0 mmol dm^{-3} respectively}. The gradient of the graph is the value of K_1^{Cl}

The visible absorption spectrum of *trans*-[Mo(CHCHMe)(η^2-MeCCH)(dppe)$_2$]$^+$ measured on the stopped-flow apparatus from the studies with HCl is shown in Fig. 5, and is clearly identical to that of the intermediate detected in the reactions with HBr. As we have already discussed, this same intermediate is also detected in the low-temperature ^{31}P-{^{1}H} NMR spectroscopy experiments. However, it is only in these studies with HCl that the detected intermediate is shown to be formed by the addition of a single proton to *trans*-[Mo(η^2-MeCCH)$_2$(dppe)$_2$].

The values of K_1^{Cl} and K_1^{Br} must differ by at least a factor of 100 (Table 2). This difference in the protonation constants is a consequence of the different acid strengths of essentially undissociated HCl and HBr in thf.[15]

The absorbance–time curve to form *trans*-[MoCl(CHCHMe)(dppe)$_2$] can be fitted by a single exponential at all acid concentrations, indicating that the reaction exhibits a first-order dependence on the concentration of complex. This conclusion is confirmed by studies at a constant concentration of acid, [HCl] = 10.0 mmol dm^{-3}, while the concentration of complex is varied in the range, *trans*-[Mo(η^2-MeCCH)$_2$(dppe)$_2$] = 0.05–0.25 mmol dm^{-3}. Under these conditions k_{obs} = 0.22 ± 0.01 s^{-1}.

The dependence on the concentration of HCl is complicated. At high concentrations of HCl the rate of reaction exhibits a linear dependence on the concentration of HCl, but at low concentrations of HCl the values of k_{obs} are significantly lower than is predicted by extrapolation of the linear portion of this curve. The non-linear dependence on the concentration of HCl is a consequence of the equilibrium protonation of *trans*-[Mo(η^2-MeCCH)$_2$(dppe)$_2$] at low concentrations of acid. Thus, in analysing the kinetics with HCl the full form of the rate law shown in equation (4) must be used. However, one simplification is possible since even at the highest values of HCl studied, k_{obs} always exhibits a linear dependence on the concentration of acid, and thus the last term in the denominator of equation (3) can be neglected, to give equation (5).

$$\frac{-d[Mo(\eta^2\text{-MeCCH})_2(dppe)_2]}{dt} = \frac{K_1^{Cl}[HX]\{k_3 + K_2^{Cl}k_4[HCl]\}}{1 + K_2^{Cl}[HCl]} \times [Mo(\eta^2\text{-MeCCH})_2(dppe)_2] \quad (5)$$

The dependence on the concentration of HCl can be simulated accurately over the entire acid concentration range using this equation; the value of K_1^{Cl} = 1.3 × 10^2 dm^3 mol^{-1} determined spectrophotometrically and $k_4K_2^{Cl}$ = 7.5 ± 0.5 dm^3 mol^{-1} s^{-1} calculated from the kinetic data at high concentrations of HCl. The best fit to the entire data is obtained when k_3 = 0.35 ± 0.03 s^{-1}. This value of k_3 is in excellent agreement with the value obtained in the studies with HBr (Table 2).

Formation of trans-[MoF(CCH$_2$Me)(dppe)$_2$].—The kinetics of the reaction between *trans*-[Mo(η^2-MeCCH)$_2$(dppe)$_2$] and HBF$_4$·OEt$_2$ have not been studied in as much detail as the reactions with HCl and HBr described above. There are two reasons for this: (*i*) the reaction gives a mixture which is predominantly the vinyl and alkylidyne complexes (as demonstrated by the ^{1}H NMR spectrum of the *isolated* crude product), together with some decomposition product which is removed during the initial crystallisation of the oily reaction mixture and (*ii*) the identity of the 'active' acid is not clear (both HBF$_4$ and HF are present). Over the acid concentration range, [HBF$_4$] = 1.0–20.0 mmol dm^{-3} the reaction exhibits the same absorbance–time characteristics as HBr or at high concentrations of HCl: an initial absorbance decrease complete within the dead-time of the stopped-flow apparatus, followed by a single exponential absorbance–time decay. The rate of the reaction was independent of the concentration of acid and the rate law is given by equation (6).

$$-d[Mo(\eta^2\text{-MeCCH})_2(dppe)_2]/dt = (2.75 \pm 0.3)[Mo(\eta^2\text{-MeCCH})_2(dppe)_2] \quad (6)$$

This behaviour is consistent with the mechanism shown in Scheme 1. Within the deadtime of the stopped-flow apparatus rapid diprotonation of *trans*-[Mo(η^2-MeCCH)$_2$(dppe)$_2$] gives *trans*-[Mo(CHCH$_2$Me)(η^2-MeCCH)(dppe)$_2$]$^{2+}$ (the same intermediate is formed at high concentrations of HBr), and subsequent rate-limiting dissociation of the *trans*-propyne ligand followed by attack of fluoride ion (derived from BF$_4^-$) gives *trans*-[MoF(CHCH$_2$Me)(dppe)$_2$]$^+$.

The observed kinetics for this system are consistent with the generalised rate law shown in equation (3). If both K_1^F and K_2^F are large, then both $K_1^F[HBF_4] \gg 1$ and $K_1^FK_2^F[HBF_4]^2 \gg 1$ and the limiting expression in equation (7) is obtained.

$$-d[Mo(\eta^2\text{-MeCCH})_2(dppe)_2]/dt = k_4[Mo(\eta^2\text{-MeCCH})_2(dppe)_2] \quad (7)$$

Comparison of equations (6) and (7) gives the value k_4 = 2.75 ± 0.3 s^{-1}. This value is in excellent agreement with the value of k_4 observed at high concentrations of HBr (Table 2).

Relatively rapid proton loss from the alkylidene ligand of *trans*-[MoF(CHCH$_2$Me)(dppe)$_2$]$^+$ at the carbon atom remote from the metal gives the vinyl species, *trans*-[MoF(CHCHMe)(dppe)$_2$] whereas proton loss from the carbon atom bound to the metal gives the alkylidyne complex, *trans*-[MoF(CCH$_2$Me)(dppe)$_2$].

Protonation of Co-ordinated Propyne: Formation of Vinyl or

Alkylidyne Species.—We have shown that the protonation of *trans*-[Mo(η^2-MeCCH)$_2$(dppe)$_2$] can give rise to both *trans*-[MoX(CHCHMe)(dppe)$_2$] and *trans*-[MoF(CCH$_2$Me)(dppe)$_2$]; and kinetic studies demonstrate that both species are formed by a common mechanism, involving the protonation of one propyne ligand followed by rate-limiting dissociation of the *trans* propyne ligand. Thus the product ultimately formed is not defined by the *site* of protonation but is decided by factors which operate *after* the rate-limiting dissociation step.

The alkylidyne species has only been isolated from the reaction with HBF_4·OEt_2. However, it seems likely that, irrespective of the acid, in solution an equilibrium mixture of all four complexes shown on the right hand side of Scheme 1 is present. Which product is *isolated* from this mixture will depend upon either the relative magnitudes of the three equilibrium constants interconnecting these four species or merely the relative solubilities of each complex.

In terms of the relative positions of the three equilibria, it seems unlikely that the fluoro-ligand favours deprotonation at the carbon atom adjacent to the metal, whereas a chloro- or bromo-ligand favours deprotonation of the carbon atom remote from the metal. Earlier studies on the two series of complexes *trans*-[Mo(NH)X(dppe)$_2$]$^+$ and *trans*-[Mo(NNH$_2$)X(dppe)$_2$]$^+$ (X = F, Cl or Br)[17,18] showed that protons on nitrogen atoms, both adjacent and remote from the metal, are *less* acidic in the fluoro-complexes than in the analogous chloro- or bromo-species, and it seems likely that similar effects operate in the carbon-based residues bound to the {Mo(dppe)$_2$} site. Therefore, it seems most likely that the relative *solubilities* of the products define which product is isolated.

Stereochemistry of the Product and Relevance to Stereoselective Alkene Formation.—Previously we have discussed how the initial site of protonation of alkyne complexes defines the stereochemistry of the derived vinyl ligand.[9] Thus, initial protonation at the metal followed by intramolecular migration onto the co-ordinated propyne would give a *trans*-vinyl ligand, whereas direct proton attack at the propyne would give a *cis*-vinyl species. The proton–proton coupling constants observed in the ^{1}H NMR spectrum of *trans*-[MoBr(CHCHMe)(dppe)$_2$] indicate a *cis* stereochemistry for the vinyl ligand, apparently consistent with the mechanism shown in Scheme 1, involving direct protonation at the propyne. However, this result is misleading and the observed stereochemistry is not dictated by the initial site of protonation in this case. At high concentrations of HBr the dominant protonation pathway involves *trans*-[MoBr(CHCH$_2$Me)(dppe)$_2$]$^+$. The presence of the carbon–carbon single bond in this species (and its precursors) permits essentially free rotation about this bond. This free rotation results, in principle, in a mixture of *cis* and *trans* vinyl ligands upon proton loss. Clearly, the isolation of *trans*-[MoBr(CHCHMe)(dppe)$_2$], containing a *cis* vinyl ligand, must reflect a significant difference in thermodynamic stability or solubility between the *cis*- and *trans*-vinyl species. That is, in this case, the *cis*-vinyl stereochemistry is thermodynamically controlled.

This observation is important in understanding the formation of stereospecific alkenes by protonation of co-ordinated alkynes both in simple complexes and the metalloenzyme, nitrogenase.[18] It has already been shown in species such as [V(η^5-C$_5$H$_5$)$_2$(η^2-PhCCPh)]$^+$ (ref. 9) and [Nb(η^5-C$_5$H$_5$)$_2$H(η^2-PhCCPh)][19] that regiospecific protonation (metal or alkyne) results in a stereospecific vinyl species. Subsequent, further regiospecific protonation of the vinyl ligand at the carbon atom adjacent to the metal gives the corresponding stereospecific alkene. Thus in these systems the stereoselectivity is kinetically controlled. The work described in this paper indicates that the stereoselective formation of an alkene by protonation of a co-ordinated alkyne can be accomplished by *thermodynamic* control. Protonation of a stereospecific vinyl ligand at the carbon atom remote from the metal generates an alkylidene species and subsequent deprotonation produces an equilibrium mixture of *cis*- and *trans*-vinyl residues. Further protonation of this mixture will often result in a mixture of isomeric alkenes. However, a stereospecific alkene *can* be produced from this isomeric mixture provided: (*i*) there is a significant difference in the thermodynamic stabilities of the isomeric vinyl species and (*ii*) protonation of the vinyl complex to give the alkene is significantly slower than the proton equilibration between the vinyl and alkylidene species.

References

1 R. A. Henderson and K. E. Oglieve, *J. Chem. Soc., Chem. Commun.*, 1991, 584 and refs. therein.
2 K. E. Oglieve and R. A. Henderson, *J. Chem. Soc., Dalton Trans.*, 1991, 3295 and refs. therein.
3 K. E. Oglieve and R. A. Henderson, *J. Chem. Soc., Chem. Commun.*, 1993, 474.
4 R. A. Henderson and K. E. Oglieve, *J. Chem. Soc., Dalton Trans.*, 1994, 767.
5 M. F. N. N. Carvalho, R. A. Henderson, A. J. L. Pombeiro and R. L. Richards, *J. Chem. Soc., Chem. Commun.*, 1989, 1796.
6 R. A. Henderson, A. J. L. Pombeiro, R. L. Richards and Y. Wang, *J. Organomet. Chem.*, 1993, **447**, C11.
7 K. W. Kramarz and J. R. Norton, *Prog. Inorg. Chem.*, 1994, **42**, 1 and refs. therein.
8 R. A. Henderson, *J. Chem. Soc., Dalton Trans.*, 1995, 503.
9 R. A. Henderson, D. J. Lowe and P. Salisbury, *J. Organomet. Chem.*, 1995, 489, C22.
10 J. R. Dilworth and R. L. Richards, *Inorg. Synth.*, 1980, **20**, 126.
11 A. Hills, D. L. Hughes, N. Kashef, M. A. N. D. A. Lemos, A. J. L. Pombeiro and R. L. Richards, *J. Chem. Soc., Dalton Trans.*, 1992, 1775 and refs. therein.
12 R. A. Henderson, *J. Chem. Soc., Dalton Trans.*, 1982, 917.
13 See, for example, R. G. Wilkins, *Kinetics and Mechanism of Reactions of Transition Metal Complexes*, 2nd edn., VCH, Weinheim, 1991, p. 11.
14 R. A. Henderson and K. E. Oglieve, *J. Chem. Soc., Dalton Trans.*, 1993, 3431.
15 S. F. Dyke, A. J. Floyd, M. Sainsbury and R. S. Theobald, *Organic Spectroscopy*, Penguin, Harmondsworth, 1971, p. 153.
16 N. Kashef and R. L. Richards, *J. Organomet. Chem.*, 1989, **365**, 309.
17 J. D. Lane and R. A. Henderson, *J. Chem. Soc., Dalton Trans*, 1986, 2155 and refs. therein.
18 D. J. Evans, R. A. Henderson and B. E. Smith, *Bioinorganic Catalysis*, ed. J. Reedijk, Marcel Dekker, New York, 1993, p. 89 and refs. therein.
19 J. A. Labinger and J. Schwartz, *J. Am. Chem. Soc.*, 1975, **97**, 1596.

Received 10*th February* 1995; *Paper* 5/00808E